Stress calculation at tube-to-tubesheet joint using spring model and its comparison with beam model

Chakradhar.K.Bhande[1], Dattatray.N.Jadhav[2], Sangram.P.Powar[3]

[1]Postgraduate student, Department of Mechanical engineering Sardar Patel College of Engineering, Mumbai, India.
[2]Associate Professor, Department of Mechanical engineering Sardar Patel College of Engineering, Mumbai, India.
[3]Department Head, FEA Department of Ideametrics Private Limited, Pune, India.

Abstract: *This paper discuss about evaluation of stresses of tubesheet joint and axial deformation of shell and tubes of heat exchanger for dewaxing application under transient thermal loading. Two models of tube and tubesheet, one using tubes as beams and other using tubes as springs has been used to calculate stresses at tube and tubesheet junction. Axial deformation of shell and induced stresses at tube-to-tubesheet junction obtained by both models are in close comparison with each other but the computational solution time required for model with sprigs is almost 38% less than for model with beams.*
Keywords: *Beam Elements, Spring Rate, Transient Thermal Analysis, Tube-to-Tubesheet Joint.*

I.   Introduction

Heat exchangers are widely used in process industry. Tubesheet is the main part of the exchanger. Various researchers in many countries have done a lot of work for the calculation and design of the tubesheet [1]. Typically, the thicknesses of the shell and the channel in such an exchanger are calculated using the appropriate codes of American Society of Mechanical Engineers (ASME) Boiler and Pressure Vessel Code [2] and thickness of the tubesheet is usually computed from the formulas given in the Tubular Exchanger Manufacturers Association (TEMA) Standards [3]. The tube-to-tubesheet joint failure is very common in industries (refer Fig.1 and Fig.2, figures from web). Therefore, the strength level of the joints has a direct effect on the safety and the reliability of process plants. The results obtained from experiments and finite element analyses are presented in different references had mainly focused on the residual stresses, connection strength, and tightness of expanded joints of tube and tubesheet [4]. The fatigue strength of tube-to-tubesheet welded joints under cyclic loading was studied by different researchers [4].

The difference in shell side pressure and tube side pressure of heat exchanger will cause the mechanical stress. Temperature gradient exists widely between tube side as well as shell side. Therefore, there may be high thermal stress due to the high temperature difference in shell-side and tube-side. The thermal stress has great impact on the total stress distribution [5]. So the simulation of the temperature field is very important. By means of thermal analysis coupling with structure analysis, the distribution of temperature, stress and deformation is obtained. As tubes-and-tubesheet are very heavy components for FEA modeling, hence to simplify them for ease of solving within more reasonable time frame for analysis, tubes can be replaced by different kind of elements like bars, beams, pipe etc. [6].

Fig. 1: tube-to-tubesheet failure leads to leakage   **Fig. 2**: tube-to-tubesheet failure from tube inside
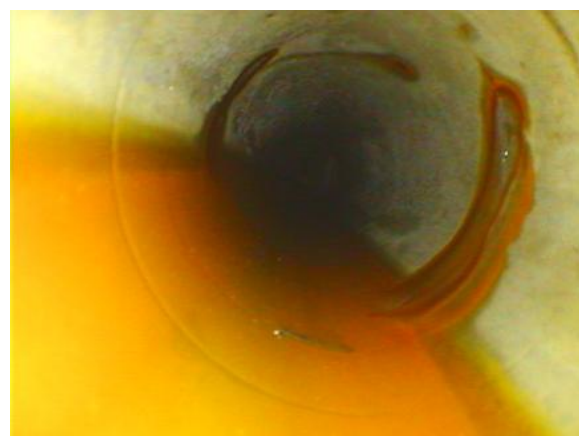
II.   Design Parameters

2.1 Loading Histogram:

The Heat Exchanger for Dewaxing application leads to transient thermal loading during its application, the detailed loading histogram is as per graph shown in Fig.3.
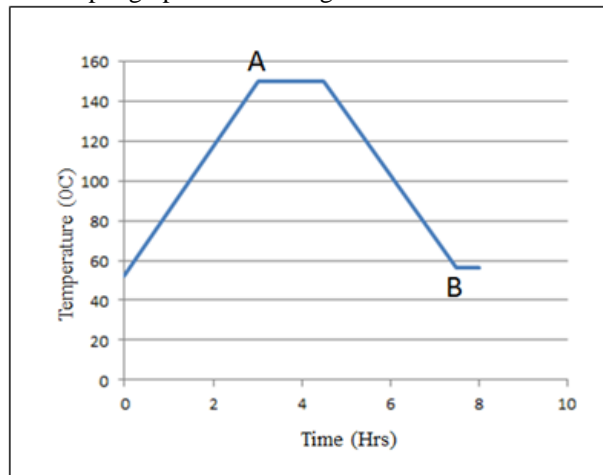
Fig. 3: thermal loading histogram for dewaxing heat exchanger [10]

2.1.1 Process Flow of Dewaxing Application [10]:

Details for dewaxing process is-
1. Heating (3Hrs): 20000 kg/h cooling medium, Inlet temperature 52°C, Outlet temperature 56.5 - 150 °C, with maximum temperature gradient of 0.5 °C/min.
2. Remelt (1.5Hrs): 20000 kg/h cooling medium, Inlet temperature 56.5°C, Outlet temperature 150 °C.
3. Cooling (3Hrs): 20000 kg/h cooling medium, Inlet temperature 56.5°C, Outlet temperature 150 –56.5°C, with maximum temperature gradient of 0.5 °C/min.
4. Stand-by (0.5Hrs): 20000 kg/h cooling medium, Inlet temperature 56.5°C, Outlet temperature 56.5 °C. No heating
5. Shell side maximum temperature is 175°C.
6. Shell side constant pressure is 1.6965 MPa and tube side constant pressure is 1.9024 MPa.

2.2 Overall geometry parameters:

Overall geometry parameters of dewaxing heat exchanger are given in Table 1.

Table 1. Overall geometry parameters of dewaxing heat exchanger [10]

Sr. No	Shell ID	Unit	Value
1	Shell Thickness	mm	7
2	Tubesheet Ref face to Face Distance	mm	2470
3	Overall Length	mm	3520
4	Corrosion Allowance (Shell Side/Tube Side)	mm	3/3 (0 on tubes)
5	Tubes (Number/OD/thickness/length)	mm	202/19.5/2.3/2500
6	Tubes (pitch/pattern)	mm	23.81/ Δ

2.3 Material properties:

Material properties for individual components subjected to temperature, are taken from ASME section II, Part D [7]. Material properties considered for coupled transient thermal and structural analysis are given in Table 2.

Table 2. Material properties with respect to temperature [7]

Shell, Channels, Dish Ends- SA 516 Gr 70 Tubesheet- SA 266 Gr 2 Tubes- SA 210 Gr A1					
Thermal conductivity		Coefficient of thermal expansion		Young's Modulus	
Temp (°C)	TC (W/m °C)	Temp (°C)	TE (mm/mm/°C)	Temp (°C)	E (MPa)
20	60.4	20	1.15E-05	25	202E3
50	59.8	50	1.18E-05	100	198E3
75	58.9	75	1.19E-05	150	195E3
100	58	100	1.21E-05	200	192E3
125	57	125	1.23E-05	250	189E3
150	55.9	150	1.24E-05	300	185E3

175	54.7	175	1.26E-05	350	179E3
200	53.6	200	1.27E-05	400	171E3

III. Finite Element Analysis

3.1 Methodology:

Heat exchanger is subjected to transient thermal loading, thermal loading is considered as per the loading histogram shown in Fig.3, two static structural analyses has been carried out at two governing points on loading histogram using results from transient thermal analysis, one at Instance A and other at instance B (refer Fig.3). Instance A is a point where heating cycle completes at time t=3Hrs and instance B is end of cooling cycle at time t=7Hrs.

In order to simplify tube-to-tubesheet model for FEA, tubes can be replaced by different kind of elements like bars, beams, pipe etc. [6]. This will significantly reduce the number of elements and allow the model to mesh and solve in a more reasonable time frame. Two different models of tubes and tubesheet one using tubes as beams and other using tubes as springs are used to calculate maximum stresses at tube and tubesheet junction.

3.2 Finite Element Model (Model 1)

Model I include both tubesheet with six numbers of solid tubes i.e. one solid tube from each pass and remaining tubes as beam elements are used to represent actual interaction between tube and tubesheet. Fig.4 shows the section view of FEA model I of tube and tubesheet with beams.

3.2.1 Loading and Boundary condition: Temperature is applied on channel side face of tubesheet as well as solid tubes considered. Tube side thermal loads from first pass through exit of six pass is calculated by linear interpolation between 1st pass compartment at 52°C and exit of sixth pass at 150°C. Shell side constant temperature of 180°C is applied on internal faces of shell, tubesheet as well as outer faces of solid tubes. Effect of insulation is modeled in this analysis by giving equivalent heat transfer coefficient [8]. Thermal loadings applied to model I are shown in Fig.5.

Fig. 4: FE model with beams- section view   **Fig. 5**: thermal loading conditions for model I
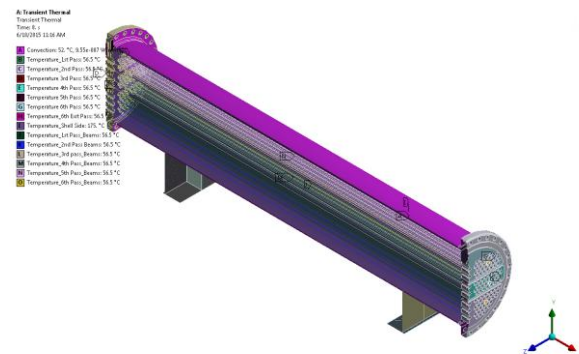
Results of transient thermal analysis are coupled with mechanical loadings which include pressure on shell side and pressure on tube side along with bolt operating load (Wm$_1$) and gasket seating load (Wm$_2$) on tubesheet. Bottom face of left saddle is fixed while right saddle has frictionless support. Bolt loads are calculated using following equations.

Operating Load, $Wm_1 = (\pi/4 * G^2) P + 2\pi bGmP$

Seating Load, $Wm2 = \pi bGy$

Where,   P = Internal design pressure = 1.9024 MPa

      G = Gasket reaction diameter = 485 mm

      b = Effective gasket width = 5 mm

      y = Gasket seating factor = 62 MPa

      m = Gasket sealing factor = 3.75

Gasket factors m and y are considered from Table 2-5.1 of ASME, Section VIII, Div. 1, Ed. 2010 [9] based on material and construction of gasket.

Fig.6 shows structural loading and boundary conditions for model I
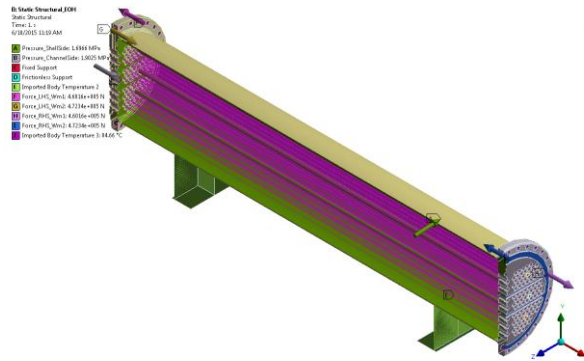
Fig. 6: structural loading and boundary conditions for model I

3.3 Finite Element Model (Model II)

Both tubesheet with six numbers of solid tubes i.e. one solid tube from each pass and remaining tubes as six springs i.e. one spring for each pass are considered in model II, In order to use the spring connectors, the applicable spring rate of the tubes is determined, so that it can maintain stiffness between tubesheet.

3.3.1 Effective spring rate:

Hooke's law for springs: $F = k*d$

But, axial displacement: $d = F*L / (A*E)$

Where,   F = Axial Force due to thermal deformation, N

k = Spring Rate, N/mm

d = Displacement, mm

L = Tube Length, mm

A = Cross Sectional Area of tube hole in tubesheet, mm^2

E = Modulus of Elasticity of tube material, MPa

By combining these equations: $d = k*d*L/ (A*E)$

Therefore, $k = (A*E) /L$

For area over tube holes equation becomes: $k = E / L$

Fig.7 shows the section view of FEA model II of tube and tubesheet with internal solid tubes and springs
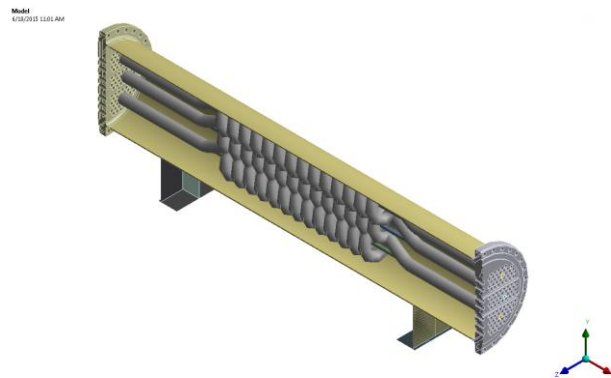
Fig. 7: FE model with springs– section view of model II

3.3.2 Loading and Boundary condition:

Loadings and boundary conditions applied to model II are same as that of model I, as there is change in only FEA model not in methodology and loading conditions. Fig. 8 and Fig. 9 shows thermal loadings and mechanical loadings for model II respectively.
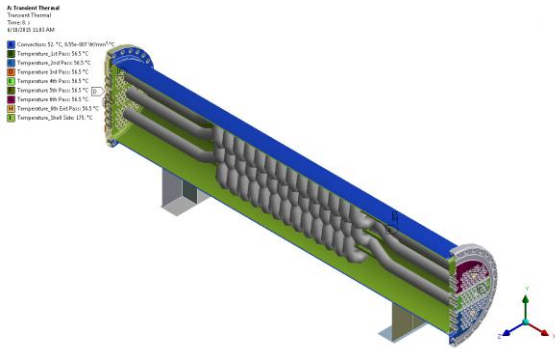
Fig. 8: thermal loading conditions for model II
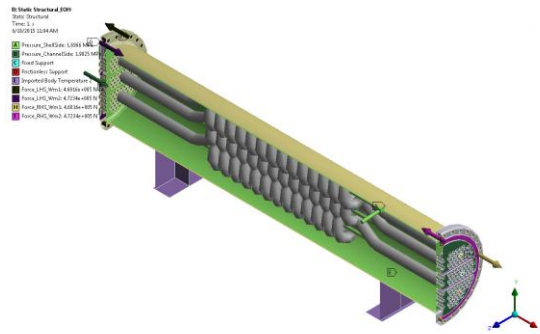
Fig. 9: structural loading conditions for model II

IV. Results and discussions

On solving both models for coupled transient thermal with two structural analysis one at the end of heating cycle (t=3Hrs) and other at the end of cooling cycle (t=7.5Hrs), maximum von mises stresses are obtained in both models. Sections 4.1 and section 4.2 represents the details of results for model I and model II.

4.1 Finite Element Analysis Results for Model I:

Maximum axial deformation of 3.8003 mm with maximum von mises stress of 279.84 MPa is induced in model I at the end of heating cycle, maximum stress is induced at tube-to-tubesheet junction, likely due to the differential thermal expansion in shell and beams. Fig.10 and Fig.11 shows axial deformation and von mises stress stress plots respectively for model I.
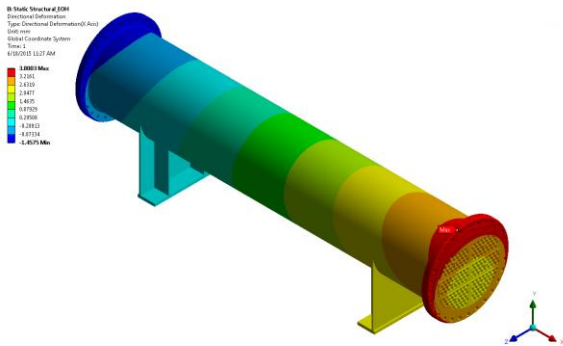
Fig. 10: axial deformation of shell
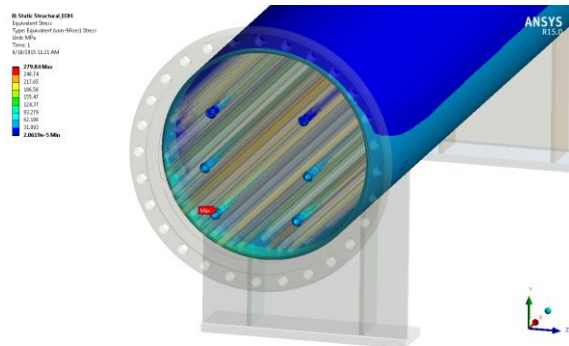
Fig. 11: von mises stress at tube-to-tubesheet junction

Similerly, Maximum axial deformation of 3.5616 mm with maximum von mises stress of 253.79 MPa is induced in model I at the end of cooling cycle, at tube-to-tubesheet junction. Results for model I are further summerised in Table 3.

4.2 Finite Element Analysis Results for Model II:

Maximum axial deformation of 3.8873 mm with maximum von mises stress of 315.40 MPa is induced in model II at the end of heating cycle, maximum stress is induced at tube-to-tubesheet junction, likely due to the differential thermal expansion in shell and solid tube. Fig.12 and Fig.13 shows axial deformation and von mises stress stress plots respectively for model II.
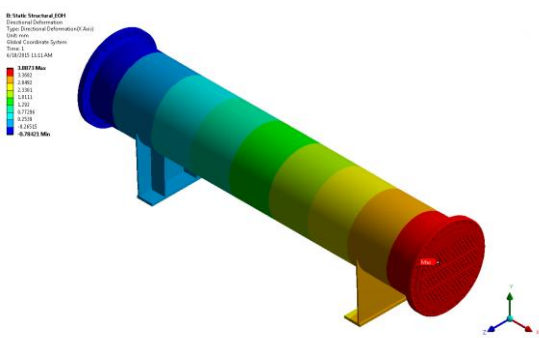
Fig. 12: axial deformation of shell
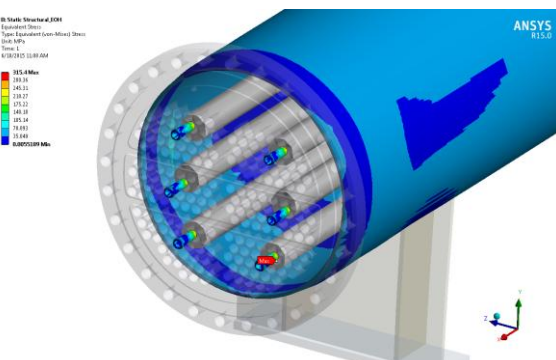
Fig. 13: von mises stress at tube-to-tubesheet junction

Similerly, Maximum axial deformation of 3.6679mm with maximum von mises stress of 268.45 MPa is induced in model II at the end of cooling cycle, at tube-to-tubesheet junction. Results for model II are further summerised in Table 3

V.   Conclusion

Maximum von mises stresses and axial deformation for coupled transient thermal and structural analysis of both models are shown in Table 3.

Table 3. Results summary for model I and model II

FEA Model	Instance (Hrs)	Model I	Model II	% Change
Maximum Axial Deformation (mm)	A (3)	3.8003	3.8873	2.29
	B (7.5)	3.5616	3.6679	2.98
Maximum Von mises Stress (MPa)	A (3)	279.84	315.4	12.71
	B (7.5)	253.79	268.45	5.78

Axial deformation of shell and maximum von mises stress induced at tube-to-tubesheet junction for these two models have minimum difference under complicated mechanical and thermal loadings, so the FEA analyses for the tubesheet with these two models are reliable.

Beam elements represent actual interaction between tubesheet and have good properties for behavior against complicated thermal and mechanical loading, but it takes approximately 38% more computational solving time than model with springs. Hence model with tubes as spring elements can be feasible to find out stresses at tube-to-tubesheet junction within reasonable time frame. Comparison of different aspects of software solver (ANSYS 15.0) for model I and model II are shown in Table 4.

Table 4. Solver output summary for model I and model II

Particular	Load Case	Model I	Model II	%Change
No. of Nodes		3395589	3161445	6.90
No. of Elements		2148464	2031066	5.46
Time required for solution (Hrs)	Transient Thermal	4.17	3.63	12.95
	Structural Analysis	9.26	4.75	48.70
	Total Time	13.43	8.38	37.60
Memory used (GB)	Transient Thermal	10.82	10.34	4.44
	Structural Analysis	25.31	23.94	5.41

The system configuration used for analysis of both model is-
Processor: Intel(R) Xeon(R) CPU E5-2630 v3 @ 2.40GHz.
RAM: 32.0 GB. System type: 64-bit operating system, X64-based processor.

References

[1].   Ming-De X., The Basis of Tubesheet Design Rules in the Chinese Pressure Vessel Code, Pressure Vessel Piping 186:13–20, 1990.
[2].   ASME. ASME Boiler and Pressure Vessel Code, 2010 Edition, the American Society of Mechanical Engineers - New York, 2010.
[3].   TEMA, Standard of Tubular Exchanger Manufactures Association, 9th Edition, Tubular Exchanger Manufactures Association, 2007.
[4].   Wenxien Su Ning Maa, Zhifu Sang and G.E.O. Widera, Investigation of Fatigue Strength of Welded Tube to Tubesheet Joint, Journal of Pressure Vessel Technology, vol. 131, pp 041205/1-5, August 2009.
[5].   W. Reinhardt and R. Kizhatil, Analysis of a Tubesheet Undergoing Rapid Transient Thermal Loading, Journal of Pressure Vessel Technology, vol. 122, pp. 476-481, November 2000.
[6].   Weiya Jin and Zengliang Gao, Comparison of two FEA models for calculating stresses in shell-and-tube heat exchanger, International Journal of Pressure Vessels and Piping 81 (2004) 563–567, 2004.
[7].   ASME. ASME Boiler and Pressure Vessel Code, Section II, Part D (metric), 2010 Edition, The American Society of Mechanical Engineers - New York, 2010.
[8].   J.P. Holman, Heat Transfer Sixth edition, Equation 2-15, Table1 -2.
[9].   ASME. ASME Boiler and Pressure Vessel Code, Section VIII, Div. 1. 2010 Edition, the American Society of Mechanical Engineers - New York, 2010.
[10].   Design data, geometric parameters and loading histogram are taken from Ideametrics Pvt. Ltd. Pune, India.